

Tunable pulsed vacuum ultraviolet light source for surface science and materials spectroscopy based on high order harmonic generation

D. Riedel, J. L. Hernandez-Pozos, R. E. Palmer, S. Baggott, K. W. Kolasinski et al.

Citation: *Rev. Sci. Instrum.* **72**, 1977 (2001); doi: 10.1063/1.1351835

View online: <http://dx.doi.org/10.1063/1.1351835>

View Table of Contents: <http://rsi.aip.org/resource/1/RSINAK/v72/i4>

Published by the [AIP Publishing LLC](#).

Additional information on *Rev. Sci. Instrum.*

Journal Homepage: <http://rsi.aip.org>

Journal Information: http://rsi.aip.org/about/about_the_journal

Top downloads: http://rsi.aip.org/features/most_downloaded

Information for Authors: <http://rsi.aip.org/authors>

ADVERTISEMENT



JANIS

**Janis Dilution Refrigerators & Helium-3 Cryostats
for Sub-Kelvin SPM**

Click here for more info www.janis.com/UHV-ULT-SPM.aspx

Tunable pulsed vacuum ultraviolet light source for surface science and materials spectroscopy based on high order harmonic generation

D. Riedel,^{a)} J. L. Hernandez-Pozos, and R. E. Palmer

Nanoscale Physics Research Laboratory, School of Physics and Astronomy, The University of Birmingham, Edgbaston, Birmingham B15 2TT, United Kingdom

S. Baggott and K. W. Kolasinski

School of Chemistry, The University of Birmingham, Edgbaston, Birmingham B15 2TT, United Kingdom

J. S. Foord

Physical and Theoretical Chemistry, University of Oxford, South Parks Road, Oxford, South Parks Road, Oxford OX1 3QZ, United Kingdom

(Received 29 August 2000; accepted for publication 22 December 2000)

We report here the development of a tunable vacuum ultraviolet light source, providing subpicosecond pulses over the wavelength range from 114 (~11 eV) to 32 nm (~39 eV), designed for surface science experiments. The source is based on high order harmonic generation. The experimental setup is described in detail and the harmonic yield as a function of the gas type (xenon or argon) is compared with theoretical descriptions. We address in particular the tunability of the source, desirable for surface science applications. Absolute characterization of the harmonic yield has also been performed and validated with time-resolved fluorescence measurements. The results are extremely promising, with intensities of $\sim 10^{10}$ photons/s, with regard to the use of this coherent source for surface science and spectroscopy. © 2001 American Institute of Physics.

[DOI: 10.1063/1.1351835]

I. INTRODUCTION

Progress in the field of surface science has often arisen from the development of novel experimental tools. For example, the interaction between surfaces and electromagnetic radiation in the vacuum ultraviolet (VUV) range is now mainly performed at synchrotron facilities. However, while offering outstanding flux and brilliance, these sources are not, in general, on site and especially do not provide subpicosecond pulses. One exciting area of surface science that would benefit especially from the availability of tunable VUV radiation in the laboratory is surface photochemistry.¹ Many molecules absorb light strongly between 6 and 40 eV. Moreover, in this energy window, where the photon energy exceeds the work function of the substrate, the generation of photoelectrons can drive completely new channels for photodissociation.²

The natural question that emerges is whether a compact (tabletop) and tunable VUV source, with enough photon flux to be used in surface science studies, can be built. The current state of the art in tabletop optical technology offers us three main options³ by which to generate VUV wavelengths: (i) plasma-based sources, (ii) VUV/xuv (extreme ultraviolet) (x ray to ultraviolet) lasers, and (iii) high order harmonic generation.

Plasma-based sources offer the promise of a high yield of photons; however as they are, of course, based on the recombination lines of the laser-produced plasma (together with a broad blackbody background), the availability of dif-

ferent wavelengths is limited. Careful optimization of a number of parameters would be needed. Additionally, for those applications in which coherent radiation is needed this type of source is not an option. Note that plasma sources offer good qualities for 13 nm lithography.⁴

VUV and XUV lasers also offer a high photon yield and very high peak power.^{5,6} Usually these systems have better performances for wavelengths <30 nm and have limited tunability. But the main drawback of this kind of system as a light source for surface science is its very low repetition rate of only a few shots per hour.

A source based on high order harmonic generation (HHG) will generate wavelengths corresponding to the odd harmonics of the pump beam.^{7,8} A monochromator can select particular harmonics, and the wavelength of the pump laser can also be tuned. A remarkable characteristic of high order harmonic generation is that most of the harmonics are produced with very similar intensities and subpicosecond pulse width.⁹⁻¹² Although the efficiency of the HHG process is relatively weak (typically 10^{-5} – 10^{-8}), the latest laser technology suggests it should be feasible to obtain sufficient flux (photons) per pulse to use this kind of device as a coherent light source for experiments in atomic, molecular, and solid state physics. Indeed, several applications of HHG have now developed from the groups whose main research lies in laser physics and VUV source characterization. These include time-resolved spectroscopy of gas phase species and electron density measurement in solids.^{13,14}

In this article, we describe the development of a tunable VUV source (10–40 eV) for surface science and spectroscopy based on HHG. The semiclassical model of HHG is

^{a)}Electronic mail: damien@nprl.ph.bham.ac.uk

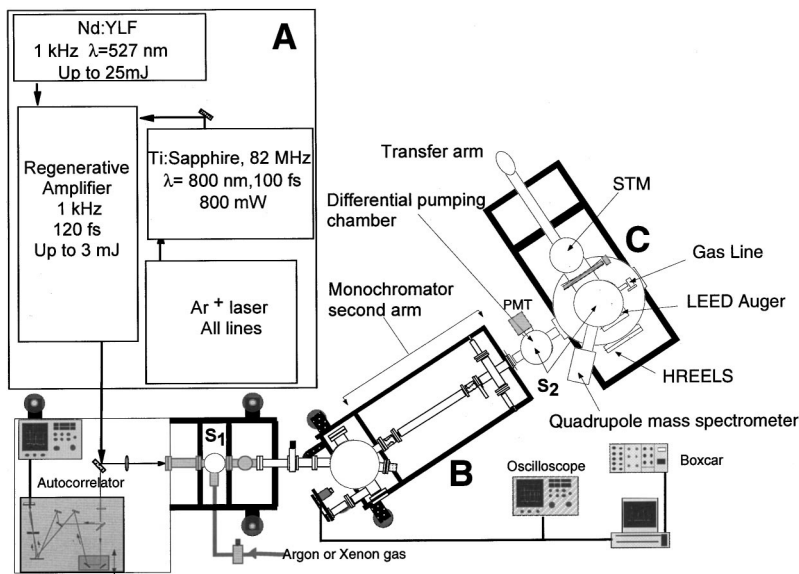


FIG. 1. Schematic of the VUV light source. The commercial femtosecond (A) laser system generates a pulse train (2.7 mJ, 800 nm, 120 fs with a repetition rate of 1 kHz) that gives intensities of $I \sim 1.6 \times 10^{14} \text{ W cm}^{-2}$ after focusing. The interaction of this very high peak power IR beam with a gas jet yields photons with energies from 10 to 40 eV which are selected via the monochromator (B). A differential pumping chamber and an UHV sample analysis chamber (C) are located in the axis of the monochromator in order to irradiate the surface system with VUV photons.

reviewed in Sec. II. In Sec. III we describe the setup of our source. The way in which the design criteria were influenced by the application is discussed. In Sec. IV, we summarize the source performance for the two rare gases (Ar and Xe) we have used to produce harmonics. In Sec. V we describe the method we have employed to measure the absolute VUV photon yield while in Sec. VI we demonstrate a first application of the source in spectroscopy, specifically with the time-resolved fluorescence decay of polyethylene terephthalate (PET) and sodium salicylate, the scintillators we have used to measure the harmonic yield.

II. HIGH ORDER HARMONIC GENERATION: REVIEW OF THEORY

The very high peak power applied in the process of high harmonic generation, typically in a rare gas flow, induces multiphoton ionization (MPI) as well as tunnel ionization (TI).¹⁵ The ratio between the two processes is often described by the Keldysh γ parameter¹⁶ where a competition between MPI and TI occurs as the wavelength and the intensity (and therefore the pulse duration) varies. In our experimental conditions, the highest harmonic order N_{max} that can be reached is described by

$$N_{\text{max}} = \frac{I_p + 3.17U_p}{h\nu}, \quad (1)$$

where $h\nu = 1.55 \text{ eV}$ is the fundamental photon energy and U_p represents the ponderomotive energy, the energy that the free electron can acquire in the laser field after tunneling. The coefficient 3.17 in Eq. (1) arises from theoretical approximation.¹⁷ U_p is described by

$$U_p = \frac{E^2}{4\omega^2}. \quad (2)$$

Here E is the electric field amplitude (V cm^{-1}) and ω is the fundamental laser frequency. The harmonic yield, for lower orders ($N=3$ and 5) is relatively high and can be described by perturbation theory.¹⁸ The intensities of the higher order harmonics follow an approximately constant conversion ef-

iciency (the ‘‘plateau’’ regime) that cannot be explained by this theoretical approach. Furthermore, it appears that the experimental cut-off energy of the plateau is often better fitted by using a lower coefficient for the U_p term.^{19,20} The intensity of the harmonics increases when the TI process is enhanced. This occurs for low frequency and high intensities where $\gamma = \sqrt{I_p/2U_p}$ is below 1, and leads to coherent high harmonic emission in the case of a single atom.¹⁶

III. EXPERIMENTAL DESCRIPTION OF THE SOURCE

Figure 1 shows a schematic of the light source. For purposes of explanation, the source can be divided into three sections: (i) the laser system (A), (ii) the HHG and monochromator chambers (B), and (iii) the ultrahigh vacuum (UHV) surface science chamber (C).

(i) The lasers we use to drive the high harmonics process are commercially available systems (Spectra Physics). A continuous wave (cw) argon ion laser (Beamlok 2060) laser pumps a Ti:sapphire laser (Tsunami, pulse duration of 100 fs, repetition rate of 82 MHz) with a 6 W multiline beam. The mode-locked Ti:sapphire laser seeds a regenerative amplifier (Super Spitfire) delivering 600 mW at around 800 nm. A laser spectrum analyzer (Rees) monitors the spectral pulse shape [full width at half maximum (FWHM) $\sim 9 \text{ nm}$]. A fourth laser, a Nd:YLF laser (Super Merlin), intracavity laser doubled by a LBO (Lithiumtriborate) crystal, delivers 25 W at 527 nm and a 1 kHz repetition rate. The Q -switched cavity yields 250 ns pulse duration with horizontal polarization. This beam pumps the two Ti:sapphire rods of the Super-Spitfire system. The regenerative amplifier is a chirped pulse amplifier (CPA) composed of a 250 ps stretcher, a multipass regenerative amplifier, and a two-stage rod amplifier followed by a compressor. This versatile system delivers a laser beam of 2.7 mJ at 800 nm with a pulse duration of $\sim 120 \text{ fs}$.

(ii) The 800 nm near-infrared beam is sent to a convex quartz lens ($f=50 \text{ cm}$) to be focused into a 500 μm diam hole through a hollow stainless steel tube, through which rare gas flows at variable pressure. The gas is recycled via a reservoir. The gas line can be fed either with xenon or argon.

The vacuum chamber housing this unit is mechanically pumped ($p \sim 10^{-3}$ mbar) and separated from the vacuum monochromator chamber by a 500 μm diam pinhole. The tube in which the gas flows is mounted on a X - Y translation stage, so that interaction area between the beam and the gas can be adjusted to manage phase matching and thus optimization of the harmonic generation process. In our experimental conditions, the $1/e$ beam diameter before the lens is $2w_s = 0.7$ cm. Therefore the beam waist at the focal point is $w_0 = (f\lambda/\pi w_s)$ TDL (where TDL is the so-called time diffraction limit). The laser beam operates at 1.5 TDL, thus giving a beam waist of $2w_0 \sim 110$ μm and a confocal parameter $b \sim 2.3$ cm at the focal point. This means an intensity of $I_p = 1.6 \times 10^{14}$ W cm^{-2} . The fundamental beam and the harmonics propagate, after emission from the tube, in the same direction towards the grating of the monochromator. The grating we use is a platinum coated (400 \AA) spherical concave silica grating ($R \sim 3$ m) with a density of 1000 grooves/mm. The zero order incidence direction is 71° while the grating holder is able to rotate $\pm 7^\circ$ around this position. This design allows us to select wavelengths from zero order down to 110 nm and therefore to observe harmonics from the seventh (H7) out to the cutoff. Because of the spherical shape of the grating the beam has some astigmatism. The tangential focal surface is situated on the external vertical slit S_2 plane of the monochromator, while the entrance slit S_1 corresponds to the plane where the fundamental beam is focused into the gas. The length of the entrance arm of the monochromator can be varied in order to adjust the energy density applied to the sample ~ 50 cm away from the exit slit and localized in a third UHV chamber. Nevertheless, we are limited by the divergence of the fundamental beam, which is directly linked by the focal length of the lens we use to focus it into the gas. Actually we have chosen to work with a 1 m arm length to simplify characterization of the harmonic yield observed. Finally, because the grating is not a variable step grating, the position of the tangential focal plane varies according to the harmonic wavelength selected by about ± 10 cm on either side of the exit slit plane.

(iii) The UHV surface science chamber contains a sample holder fixed to a cold finger that allows samples temperature from 27 to 1300 K to be reached. The cryogenic temperatures allow physisorbed systems (e.g., $\text{O}_2/\text{graphite}$) to be investigated as well as chemisorbed systems [e.g., molecules adsorbed on Si(100)-(2 \times 1) or Si(111)-(7 \times 7)]. A differential pumping system, with a 600 ls^{-1} turbopump and two horizontal pinholes, connects the monochromator ($P \sim 10^{-7}$ mbar) to this UHV sample chamber ($P \sim 10^{-10}$ mbar). This intermediate chamber is also equipped with a three-axis translation stage, which holds a retractable mirror to allow off-axis detection of the harmonic yield. The UHV sample analysis chamber is divided into two parts: the lower chamber is equipped with a spectrometer for high resolution electron loss spectroscopy (HREELS) (LK2000), a pulse-counting quadrupole mass spectrometer (Hiden), and a port allowing entry of the high harmonic beam. The upper chamber has a gas line with a leak valve system for gas dosing, a low energy electron diffraction (LEED) system for surface characterization, and a sample transfer system to

move the sample into a scanning tunneling microscope (STM) for structural analysis on the atomic scale. The main sample holder is mounted on a rotatable X - Y - Z manipulator, which permits precise placement of the sample in either the upper or lower chamber. This combination of techniques provides a powerful battery of tools for studies of surface photochemistry driven by VUV light.

IV. EXPERIMENTAL PERFORMANCE OF THE SOURCE

The first step in evaluating the utility of the VUV source in applications such as photodesorption studies or surface modification has been to characterize the harmonic yield we are able to generate and to optimize the experimental conditions. Detection of the VUV emission is performed with two kinds of scintillator. The first is a quartz window coated with a homogeneous sodium salicylate film. The second is a polymer film, PET, fixed on the same kind of quartz window. Both scintillators emit fluorescence in the blue at around 420 nm with a quantum efficiency for the sodium salicylate equal to unity²¹ when the excitation energy varies from 3.5 to 35 eV. The flange supporting the scintillator is fixed 20 cm from the exit slit to avoid rapid damage or aging due to tight focused light. A photomultiplier tube (PMT) (Hamamatsu R5600U-6) detects the fluorescence yield behind the coated windows. A blue filter (Schott BG-39) is placed in front of the PMT. The PMT is connected to a 1 GHz amplifier (EG&G model 9327), an oscilloscope, and a boxcar integrator. To deal with undesired scattered light in the second arm of the monochromator due to the infrared and the third harmonic (266 nm) beams, it was crucial to place rectangular apertures in the second arm of the monochromator. A computer controls the stepper motor board of the grating chamber and the detected, averaged signal via a 12 bit acquisition board (Advantech PCL 812 PG).

A. High order harmonic generation in xenon and argon

The ionization potential of xenon is ~ 12.2 eV. We can therefore hope to reach the order $N_{\text{max}} = 19$ (~ 29.5 eV) under our experimental conditions with this gas. Figure 2 shows a spectrum obtained for the operating conditions described in Sec. III with a ~ 20 mbar gas pressure in the flow tube. It is clear that the spectrum obtained has a plateau and shows emission from $N = 7$ to 19. Because the ionization potential of argon is ~ 15.8 eV, this gas needs greater pump intensities than xenon to obtain good conditions for harmonic generation. Figure 3 presents a typical harmonic spectrum obtained in a flow of argon with a pressure of ~ 40 mbar. The highest harmonic order obtained is the 25th, giving a cut-off value of ~ 41.9 eV; for an U_p coefficient of 3.0 the theoretical value of the cut-off energy is ~ 43 eV or H27. The two lines between the seventh and the ninth order harmonics are situated at 104.3 and 95.9 nm, and correspond to third order diffraction of H23 (34.8 nm) and H25 (32.0 nm), respectively, by the grating. The two lines between the 9th and the 11th order harmonics are situated at 84.1 and 76.2 nm and correspond to 2nd order diffraction of H19 and H21, respectively, by the grating. Furthermore, the three other lines, located at 69.5,

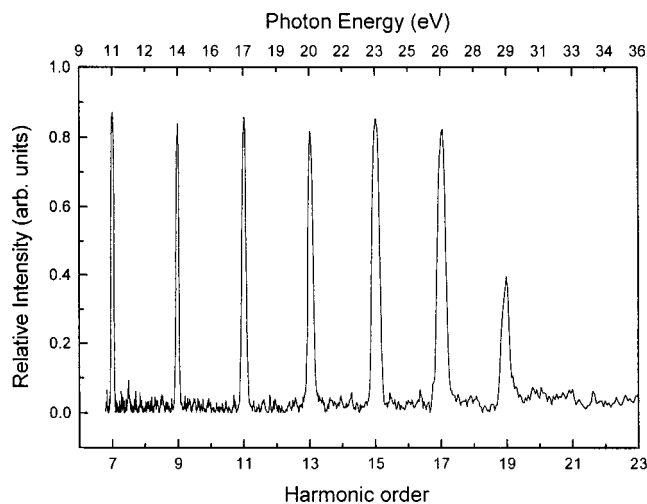


FIG. 2. High order harmonic spectrum obtained by HHG in a xenon gas jet. The gas pressure is $p \sim 20$ mbar and the IR intensity is $I \sim 1.4 \times 10^{14} \text{ W cm}^{-2}$. The scintillator used for this measurement was sodium salicylate.

64, and 59.3 nm, correspond to 2nd order diffraction of the 23rd, 25th, and 27th harmonics, respectively. It is quite clear from Fig. 3 that the harmonic order number 27 is slightly screened by the side of the grating when its rotation angle gives a better grazing incidence. Nevertheless, the presence of the second and third order reflections shows a very intense and efficient conversion process leading to significant harmonic yield. By tuning the Ti:sapphire laser around 800 nm we were able to shift these reflections (see Sec. IV B) and therefore to confirm the origin of these spectral lines. Finally, we have also noticed a weak emission centered at 93.7 nm. This last peak could correspond to the Ar II line from the $3s^2 3p^5 - 3s 3p^6$ configuration centered at 932 Å.

B. Tunability of the source

While the first level of wavelength selection in surface science experiments would be to choose a particular har-

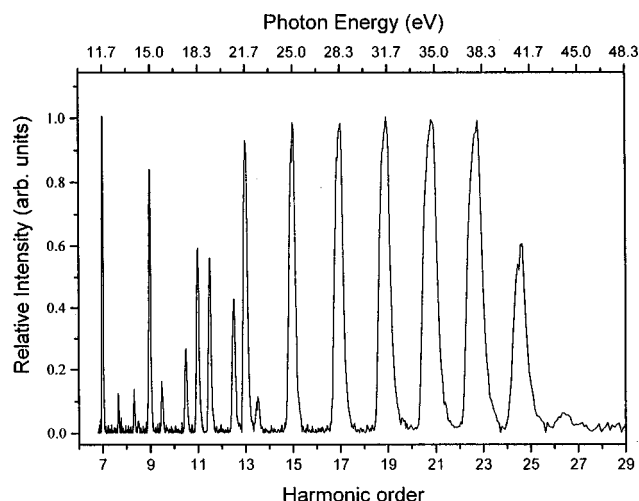


FIG. 3. High order harmonic spectrum obtained by HHG in an argon gas jet. The gas pressure is $p \sim 40$ mbar and the IR intensity is $I \sim 1.6 \times 10^{14} \text{ W cm}^{-2}$. The scintillator used for this measurement was sodium salicylate.

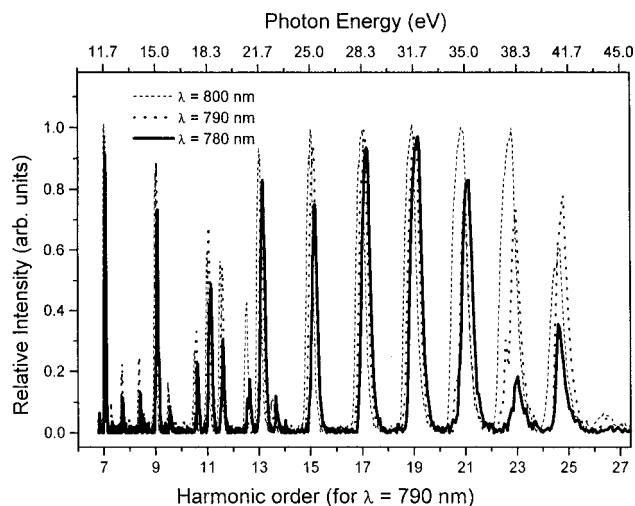


FIG. 4. Tunable high order harmonic spectrum obtained by HHG in argon. The wavelength of the oscillator laser (Ti:sapphire) is tuned by $\Delta\lambda = \pm 10$ nm about a value of 790 nm.

monic from the HHG spectrum of the source, it is quite important to obtain the highest flexibility in terms of tunability. For example, photodesorption yields can exhibit resonance structures in the photon energy domain.² As shown in Fig. 4, a relatively easy way to tune slightly the harmonic frequencies is to shift the wavelength of the pump laser. The Ti:sapphire laser we use can deliver a seed beam to the regenerative amplifier in the wavelength range from 730 to 850 nm. However, the regenerative amplifier has optical components with limited bandwidth, and they are specifically optimized for 800 nm: the tunability is therefore limited. As shown on Fig. 4, for a ± 10 nm variation around a selected wavelength of 790 nm, we can tune the observed harmonics wavelength by a value of $\Delta\lambda = 2.8$ nm (H7) to 0.8 nm (H25), corresponding to energy variations of $\Delta E \sim 0.25 - 1.04$ eV. A possible method by which to obtain a wider tunability would be to double the fundamental beam before harmonic generation in the gas, and to use an achromatic doublet to focus both wavelengths (i.e., 800 and 400 nm) in the gas flow tube.²² Even order emission could therefore be produced [e.g., $H8 = 6\omega + 1(2\omega)$].

V. ABSOLUTE ENERGY CALIBRATION

Measurement of the photon flux (photons/s) of the harmonics is not a trivial problem, especially since it deals with ionizing radiation in the VUV domain. The methods for intensity calibration in the VUV have been refined over the years and are outlined in Vol. II of Ref. 3. The calibration we have performed is based on the properties of one of the scintillators used to detect the harmonic yield, sodium salicylate. This material has a quantum efficiency which varies slowly (by 5%) over a wide range of wavelengths (380–30 nm),²¹ and can therefore be calibrated with near-UV light. The calibration process involves the use of the infrared pulsed laser (Ti:sapphire set at 730 nm, 100 fs) doubled with a β -bariumborate (BBO) crystal to provide (via density filters) a low intensity pulsed beam in the UV at 365 nm. In the first step of the method, the UV average power is read on a cali-

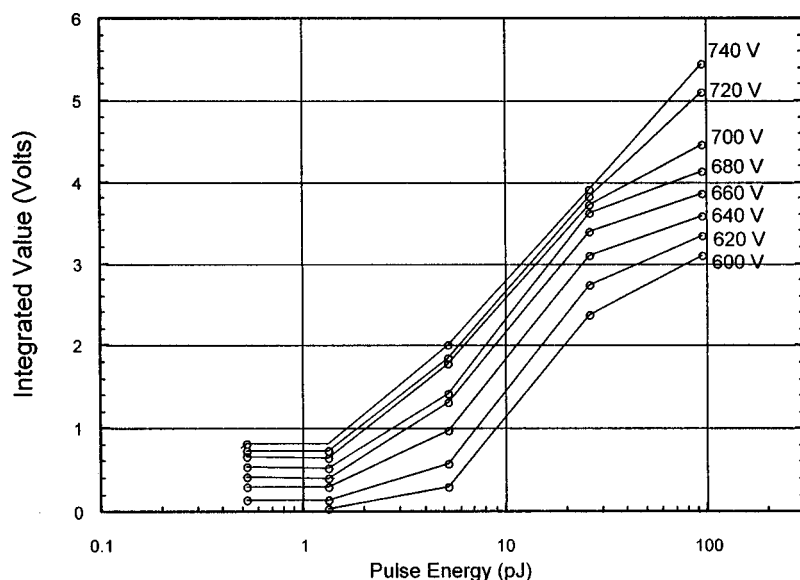


FIG. 5. Calibration curves from the boxcar voltage value to incident energy (per pulse) from VUV irradiation of a sodium salicylate scintillator. The calibration was done at 365 nm for several high voltages applied to the PMT in order to cover the full range of values needed for the VUV intensity measurement.

brated photodiode power meter for several density filters (calibrated for this wavelength) and then converted to energy values. The UV light is then directed to a quartz window [a conflat (CF) flange] coated with a thin layer (~ 0.5 – 1 mm) of sodium salicylate, behind which are a blue filter and the detection system (PMT+amplifier+boxcar averager), which measures the fluorescence of the scintillation emitted at ~ 410 nm. This gives an integrated value of the incident energy. The calibration is then made for several values of energy at 365 nm and for several voltages applied to the PMT. Thus we obtain a calibration curve (Fig. 5) relating the incident energy to the integrated signal level given by the boxcar. The VUV harmonic beam (with a pulse duration ≥ 120 fs, and broadened by the monochromator grating) is then directed upon the same calibrated scintillator coating. By keeping the same integration parameters, we are able to obtain an absolute measurement of the VUV energy or photon flux, independent of the temporal structure of the VUV pulses. Note that during the calibration of the VUV yield, the flange with the scintillator coating is directly connected to the end of the second arm of the monochromator (Fig. 1); during daily use of the source, a differential pumping vacuum chamber is instead connected at this point and the VUV yield is measured via a mirror (separately calibrated). With the calibration method described, a flux of $\sim 10^6$ – 10^7 photons/pulse of VUV radiation has been determined in the plateau region, after selection by the grating, as shown in Fig. 6 (argon). With a 1 kHz repetition rate this leads to a flux of $\sim 10^{10}$ photons/s that can irradiate the sample to be studied. Such a method gives a relative error of measurement of 10%. A quick calculation based on $\sim 10^{14}$ photons/pulse of the fundamental infrared (IR) radiation yield, with a conversion efficiency $\rho \sim 10^{-5}$ and a reflection coefficient $r \sim 10^{-2}$ of the grating, gives a typical harmonic yield of 10^7 photons/pulse, indicating that our system is working at close to optimum efficiency. Note that even after hundreds of hours of use we have noted no detectable damage of the scintillator or decrease of its efficiency, even though it is

known that some slight (5%) aging effects can occur, particularly when venting the chamber to air (scintillator oxidation).^{21,23}

VI. APPLICATIONS: SURFACE SCIENCE AND TIME RESOLVED SPECTROSCOPY

We now consider some of the possible applications of the source. Photons with energies in the region of 6–40 eV are the right energies for the absorption energy range of small molecules like CO, O₂, C₂H₄, or CO₂.^{24,25} Such simple molecules are of special interest because their thermal surface chemistry is often well established. There are still relatively few surface photodesorption studies of such molecules in the VUV,^{26–28} especially for low coverage physisorbed systems.²⁹ The processes involved can be separated in three classes: direct photoexcitation of the adsorbate with different characteristics compared with the gas phase due, principally, to selective quenching and postdissociation interactions with the substrate, the photoelectron flux induces electron stimulated reactions analogous to those observed in electron scattering processes, and a completely new channel

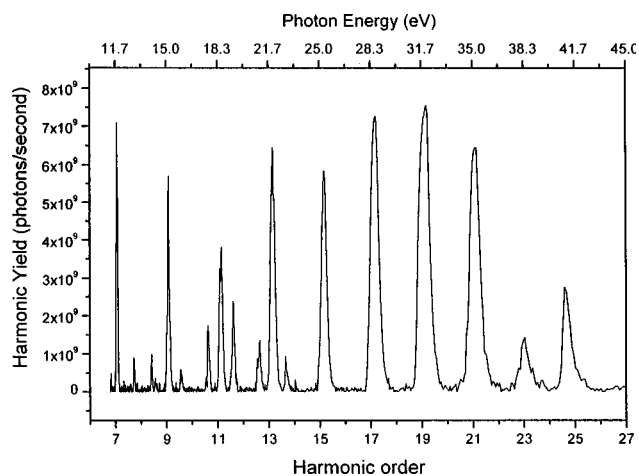


FIG. 6. Harmonic yield calibrated in intensity (photons/s) via Fig. 5.

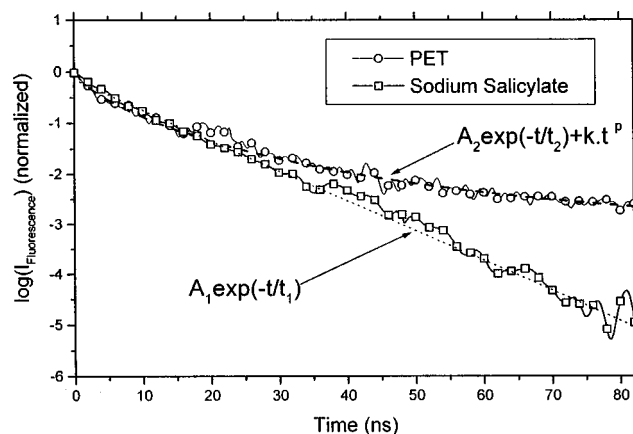


FIG. 7. Fluorescence decay curves for the two scintillators used to detect VUV photons [PET and sodium salicylate (SNa); see the text] excited at 10.85 eV (H7) with the high order harmonic source ($\sim 1 \times 10^5 \text{ W cm}^{-2}$). The SNa shows a single exponential decay ($t_1 = 8.8 \pm 0.4 \text{ ns}$) while the PET presents a nonlinear component (kt^p) induced by the VUV intensity applied.

which has been discovered by our group² in which surface electron attachment to a resonantly pumped, photoexcited molecular state occurs. The wavelength dependence of the cross section is crucial to elucidation of the mechanism in the ultrafast regime and can be addressed with a tunable HHG source. In ultrafast experiments performed with visible and near-UV photons,^{30,31} the extremely high density of excited electrons has been found to yield a unique type of process in which multiple excitations of the adsorbate take place, leading to nonlinear effects (termed “desorption induced by multiple electronic transitions” or DIMET). Direct resonant excitation of the adsorbate has not yet been demonstrated and little is known about the wavelength dependence of the photochemical dynamics. For substrate mediated reactions, power densities on the order of 900 MW/cm^2 are required to produce nonlinear effects at 310 nm.³² With the kind of VUV coherent ultrafast pulsed source described here one can obtain $\sim 0.1 \text{ MW/cm}^2$ with pulse duration on the order of 1 ps or less. While at first this suggests that the DIMET process will not be observed, the fact that, in contrast to the visible and UV, resonant molecular excitations are anticipated in the VUV, means that resonance-enhanced multiple excitation and accompanying nonlinear effects can be ruled out.

As a preliminary demonstration of the application of the VUV light source to material spectroscopy³³ we will consider briefly measurement of the fluorescence decay of the two scintillators used: sodium salicylate (SNa, $\text{C}_7\text{H}_5\text{NaO}_3$) and polyethylene terephthalate (PET, $\text{C}_{10}\text{H}_8\text{O}_4$). The first is conventionally used at synchrotrons (e.g., SuperACO, Daresbury UK) for beam detection or calibration. The second is a polymer which shows interesting electroluminescence with in the context of the development of organic light emitting diodes (OLEDs).³⁴ Both emit strong luminescence, after excitation, from the first excited singlet state (S_1, π^*), which is separated from the lower singlet state (S_0, π), by an energy of 3.04 ($\sim 410 \text{ nm}$) and 3.6 eV ($\sim 344 \text{ nm}$) for sodium salicylate and for PET, respectively. Figure 7 presents the fluorescence decay measured for both scintillators on a semi-

logarithmic scale when excited by H7 ($h\nu = 10.85 \text{ eV}$) with VUV intensity of $\sim 1 \times 10^5 \text{ W/cm}^2$. The fluorescence decay of SNa is fitted with one exponential, corresponding to an S_1 lifetime of $t_1 = 8.8 \pm 0.4 \text{ ns}$. This lifetime is known to lie between 1 and 10 ns.²³ In the case of PET, fluorescence decay is clearly not composed of a simple exponential component, and has been fitted by a combination of an exponential decay and a second nonlinear term describing a quenching process. This type of process can be linked with so-called local density induced (LDI) quenching. It has been studied in connection with the efficiency of scintillation of some inorganic crystals (e.g., NaI, CsI)³⁵ when irradiated with heavy charged particles, which exhibit this type of nonexponential decay behavior. In fact, the first part of the PET fluorescence decay, for short times ($t < 15 \text{ ns}$), is linear and corresponds to the classical exponential decay of the first singlet excited state ($t_2 = 16.2 \pm 0.6 \text{ ns}$). The second part is characteristic of delayed fluorescence due to nonlinear effects linked with the intensity applied to the polymer film (where the fitting parameters give $A_2/k \sim 3$ and $p \sim 0.8$ from $I_{\text{fluor}} = A_2 \exp(-t/t_2) + kt^p$). Such a phenomenon can occur when the density of electrons in the conduction band is high enough to produce dipole-dipole interaction with localized excitons. An in depth analysis of this behavior will be the subject of a future article. Here we emphasize two important points: (a) sodium salicylate can be used to calibrate the intensity of this kind of ultrafast VUV source; therefore the known quantum efficiency of SNa can be used, which validates our VUV yield measurement (Fig. 5, Sec. V); (b) there is clear nonlinear behavior in the relaxation of the PET when excited with VUV harmonics; the physical processes involved in this case remain to be clearly identified but this gives us a good idea of the potential for discovering new phenomena when we consider electronic excitation of materials with in the context of surface science.

ACKNOWLEDGMENTS

The authors are grateful to the EPSRC and the ERDF for financial support of this work. One of the authors (D. R.) would like to thank the European Commission for award of a Marie Curie fellowship.

- ¹W. Ho, Surf. Sci. **300**, 996 (1994); R. E. Palmer, Prog. Surf. Sci. **41**, 51 (1992); L. J. Richter and R. R. Cavanagh, *ibid.* **39**, 155 (1992).
- ²L. Siller, S. L. Bennett, M. A. MacDonald, R. A. Bennett, R. E. Palmer, and J. S. Foord, Phys. Rev. Lett. **76**, 11 (1996).
- ³J. A. Samson and D. L. Ederer, *Vacuum Ultraviolet Spectroscopy* (Academic, London, 1998), Vols. I and II.
- ⁴D. Attwood, *Soft X-rays and Extreme Ultraviolet Radiation: Principles and Applications* (Cambridge University Press, Boston, 1999).
- ⁵A. McPherson, G. Gibson, H. Jara, U. Johan, T. S. Luck, I. A. McIntyre, K. Boyer, and C. K. Rhodes, J. Opt. Soc. Am. **4**, 595 (1987).
- ⁶J. J. Rocca, Rev. Sci. Instrum. **70**, 10 (1999).
- ⁷A. L’Huillier, T. Auguste, Ph. Balcou, B. Carré, P. Monot, P. Salieres, C. Altucci, and K. S. Budil, J. Nonlinear Opt. Phys. Mater. **4**, 3 (1995).
- ⁸Z. H. Chang, A. Rundquist, H. W. Wang, M. M. Murnane, and H. C. Kapteyn, Phys. Rev. Lett. **82**, 2006 (1999).
- ⁹C. Altucci et al., Phys. Rev. A **61**, 21601 (1999).
- ¹⁰X. F. Li, A. L’Huillier, M. Ferray, L. A. Lompré, and G. Mainfray, Phys. Rev. A **39**, 5751 (1981).
- ¹¹T. Brabec and F. Krausz, Rev. Mod. Phys. **72**, 545 (2000).
- ¹²R. Bartels, S. Backus, E. Zeek, L. Misoguti, G. Vdovin, I. P. Christov, M.

- M. Murnane, and H. C. Kapteyn, *Nature (London)* **406**, 164 (2000).
- ¹³P. Cacciani, W. Ubachs, P. C. Hinnen, C. Lyngå, A. L'Huillier, and C. G. Wahlström, *Astrophys. J.* **499**, L223 (1998).
- ¹⁴D. Descamps *et al.*, *Opt. Lett.* **25**, 2 (2000).
- ¹⁵M. Levenstein, Ph. Balcou, M. Yu. Ivanov, A. L'Huillier, and P. B. Corkum, *Phys. Rev. A* **49**, 3 (1994).
- ¹⁶L. V. Keldysh, *Sov. Phys. JETP* **20**, 5 (1965).
- ¹⁷C. G. Wahlström, *Phys. Scr.* **49**, 251 (1994).
- ¹⁸D. C. Hanna, M. A. Huratic, and D. Cotter, *Nonlinear Optics of Free Atoms and Molecules* (Springer, Berlin, 1979).
- ¹⁹C. G. Wahlström, *Phys. Rev. A* **48**, 4709 (1993).
- ²⁰J. L. Krause, K. J. Schafer, and K. C. Kulander, *Phys. Rev. Lett.* **68**, 3535 (1992).
- ²¹A. Knapp and A. M. Smith, *Appl. Opt.* **3**, 5 (1964).
- ²²C. Lyngå, Thesis, Lund University, Sweden, 1999; see also Gisselbrecht *et al.*, *Phys. Rev. Lett.* **82**, 4604 (1999).
- ²³J. A. R. Samson, *Techniques of Vacuum Ultraviolet Spectroscopy* (Wiley, New York, 1967).
- ²⁴L. Siller, P. Laitenberger, R. E. Palmer, S. L. Bennett, J. S. Foord, and M. A. MacDonald, *Nucl. Instrum. Methods Phys. Res. B* **101**, 73 (1995).
- ²⁵C. M. Friedrich, J. Wilkes, R. E. Palmer, S. L. Bennett, M. A. MacDonald, C. L. A. Lamont, and J. S. Foord, *Chem. Phys. Lett.* **247**, 348 (1995).
- ²⁶A. Nilsson, O. Björneholm, H. Tillborg, B. Herdnäs, R. J. Guest, A. Sandell, R. E. Palmer, and N. Mårtensson, *Surf. Sci.* **287**, 758 (1993).
- ²⁷H. Tillborg, A. Nilsson, B. Herdnäs, N. Mårtensson, and R. E. Palmer, *Surf. Sci.* **295**, 1 (1993).
- ²⁸J. M. Coquel, T. Almeida Gasche, J. Wilkes, C. M. Friedrich, C. Lamont, M. A. MacDonald, R. E. Palmer, and A. Moutinho, *J. Phys.: Condens. Matter* **8**, 153 (1996).
- ²⁹R. A. Bennett, R. G. Sharpe, R. J. Guest, J. C. Barnard, R. E. Palmer, and M. A. MacDonald, *Chem. Phys. Lett.* **198**, 241 (1992).
- ³⁰J. A. Misewitch, T. F. Heinz, and D. W. Newns, *Phys. Rev. Lett.* **68**, 3737 (1992).
- ³¹R. R. Cavanagh, D. S. King, J. C. Stephenson, and T. F. Heinz, *J. Phys. Chem.* **93**, 786 (1993).
- ³²D. G. Busch and W. Ho, *Phys. Rev. Lett.* **77**, 1338 (1996).
- ³³R. Haight and D. R. Peale, *Rev. Sci. Instrum.* **65**, 6 (1994).
- ³⁴D. Mary, M. Albertini, and C. Laurent, *J. Phys. D* **30**, 171 (1997).
- ³⁵A. N. Belsky *et al.*, *J. Electron Spectrosc. Relat. Phenom.* **76**, 147 (1996).